

Immune correlates of protection of the four-segmented Rift Valley fever virus candidate vaccine in mice

Chittappen K. Prajeeth, Isabel Zdora, Giulietta Saletti, Julia Frieze, Thomas Gerlach, Lucas Wilken, Jana Beicht, Mareike Kubinski, Christina Puff, Wolfgang Baumgärtner, Jeroen Kortekaas, Paul J. Wichgers Schreur, Albert D.M.E. Osterhaus & Guus F. Rimmelzwaan

To cite this article: Chittappen K. Prajeeth, Isabel Zdora, Giulietta Saletti, Julia Frieze, Thomas Gerlach, Lucas Wilken, Jana Beicht, Mareike Kubinski, Christina Puff, Wolfgang Baumgärtner, Jeroen Kortekaas, Paul J. Wichgers Schreur, Albert D.M.E. Osterhaus & Guus F. Rimmelzwaan (2024) Immune correlates of protection of the four-segmented Rift Valley fever virus candidate vaccine in mice, *Emerging Microbes & Infections*, 13:1, 2373313, DOI: [10.1080/22221751.2024.2373313](https://doi.org/10.1080/22221751.2024.2373313)

To link to this article: <https://doi.org/10.1080/22221751.2024.2373313>



© 2024 The Author(s). Published by Informa UK Limited, trading as Taylor & Francis Group, on behalf of Shanghai Shangyixun Cultural Communication Co., Ltd



[View supplementary material](#)



Published online: 10 Jul 2024.



[Submit your article to this journal](#)



Article views: 556



[View related articles](#)



[View Crossmark data](#)



Immune correlates of protection of the four-segmented Rift Valley fever virus candidate vaccine in mice

Chittappen K. Prajeeth ^a, Isabel Zdora ^b, Giulietta Saletti^a, Julia Friese^a, Thomas Gerlach^a, Lucas Wilken ^{a,c}, Jana Beicht ^a, Mareike Kubinski^a, Christina Puff^b, Wolfgang Baumgärtner^b, Jeroen Kortekaas ^{d,e}, Paul J. Wichgers Schreur ^{d,f}, Albert D.M.E. Osterhaus ^a and Guus F. Rimmelzwaan ^a

^aResearch Center for Emerging Infections and Zoonoses, University of Veterinary Medicine Hannover, Foundation, Hannover, Germany; ^bDepartment of Pathology, University of Veterinary Medicine Hannover, Foundation, Hannover, Germany; ^cLeibniz Institute of Virology (LIV), Hamburg, Germany; ^dDepartment of Virology and Molecular Biology, Wageningen Bioveterinary Research, Wageningen University & Research, Lelystad, The Netherlands; ^eBoehringer Ingelheim Animal Health, Global Innovation, Saint Priest, France; ^fBunyaVax B.V., Lelystad, The Netherlands

ABSTRACT

Rift Valley fever (RVF) is a mosquito-borne zoonotic disease caused by RVF virus (RVFV). RVFV infections in humans are usually asymptomatic or associated with mild febrile illness, although more severe cases of haemorrhagic disease and encephalitis with high mortality also occur. Currently, there are no licensed human vaccines available. The safety and efficacy of a genetically engineered four-segmented RVFV variant (hRVFV-4s) as a potential live-attenuated human vaccine has been tested successfully in mice, ruminants, and marmosets though the correlates of protection of this vaccine are still largely unknown. In the present study, we have assessed hRVFV-4s-induced humoral and cellular immunity in a mouse model of RVFV infection. Our results confirm that a single dose of hRVFV-4s is highly efficient in protecting naïve mice from developing severe disease following intraperitoneal challenge with a highly virulent RVFV strain and data show that virus neutralizing (VN) serum antibody titres in a prime-boost regimen are significantly higher compared to the single dose. Subsequently, VN antibodies from prime-boost-vaccinated recipients were shown to be protective when transferred to naïve mice. In addition, hRVFV-4s vaccination induced a significant virus-specific T cell response as shown by IFN- γ ELISpot assay, though these T cells did not provide significant protection upon passive transfer to naïve recipient mice. Collectively, this study highlights hRVFV-4s-induced VN antibodies as a major correlate of protection against lethal RVFV infection.

ARTICLE HISTORY Received 15 April 2024; Revised 5 June 2024; Accepted 22 June 2024

KEYWORDS RVFV; immunogenicity; T cells; antibodies; vaccines

Introduction

Rift Valley Fever virus (RVFV), a member of the genus Phlebovirus in the order *Bunyavirales* causes severe hepatitis which is especially lethal to young ruminants and abortion storms in sheep herds are typical hallmarks of RVFV epizootics [1–3]. *Aedes* and *Culex* mosquitoes are capable of transmitting RVFV primarily among cattle and also to humans. Humans exposed to contaminated body fluids or tissues are at high risk of contracting the virus [3]. Human infections are usually asymptomatic or run a mild self-limiting course with fever and flu-like symptoms. Nevertheless, 1–2% of RVFV-infected humans develop more severe complications including loss of vision, encephalitis or haemorrhagic fever, the latter with 50% case fatality rate [2]. While a human vaccine is not available, inactivated and live-attenuated vaccines (LAVs) are used to protect livestock from severe disease. However,

reports of teratogenic effects and abortions associated with the use of LAVs in animal models have precluded their routine use [4–6].

The RVFV RNA genome comprises three segments named after their size, large (L) medium (M) and small (S). The RVFV L segment encodes the viral RNA-dependent RNA polymerase, whereas the M segment encodes a polyprotein which is cleaved into the structural glycoproteins Gn and Gc. Additionally, M segment encodes a small 14-kDa protein, named NSm, and a large glycoprotein (LGp) encoded by the NSm and Gn coding regions [7–10]. The S segment encodes the nucleocapsid (N) protein and another non-structural protein (NSs), which is the major virulence factor capable of counteracting the host innate immune response primarily by antagonizing the antiviral type-I interferon response [11].

A great amount of knowledge pertaining to the immunity to RVFV following vaccination or natural

CONTACT Guus F. Rimmelzwaan guus.rimmelzwaan@tiho-hannover.de Research Center for Emerging Infections and Zoonoses, University of Veterinary Medicine Hannover, Foundation, Bünteweg 17, Hannover 30559, Germany

Supplemental data for this article can be accessed online at <https://doi.org/10.1080/22221751.2024.2373313>

© 2024 The Author(s). Published by Informa UK Limited, trading as Taylor & Francis Group, on behalf of Shanghai Shangyixun Cultural Communication Co., Ltd. This is an Open Access article distributed under the terms of the Creative Commons Attribution-NonCommercial License (<http://creativecommons.org/licenses/by-nc/4.0/>), which permits unrestricted non-commercial use, distribution, and reproduction in any medium, provided the original work is properly cited. The terms on which this article has been published allow the posting of the Accepted Manuscript in a repository by the author(s) or with their consent.

infection has come from animal studies [12–14]. These studies demonstrated that virus neutralizing (VN) antibodies targeting the viral glycoproteins Gc and Gn which are crucial for cell attachment and fusion, correlated with protection, while the role of T cells is less well established [15].

We have previously shown that splitting the M segment of RVFV into two M-type segments, each encoding one of the glycoproteins, Gn or Gc, resulted in a four-segmented variant that is highly attenuated [16]. Splitting of the M segment was expected to complicate genome packaging and generate an imbalance in glycoprotein expression. Indeed, all four-segmented variants created to date, including the variants expressing NSs were shown to be avirulent [16]. Nevertheless, to optimize its safety profile, the NSs gene was deleted, and the safety and immunogenicity of the corresponding vaccine, referred to as hRVFV-4s, has been demonstrated in various mammalian species [17–19]. In the present study, we confirm the protective efficacy of hRVFV-4s immunization in a mouse model of severe RVF disease and in addition define correlates of protection by executing passive transfer experiments.

Materials and methods

Ethical statement

Approval to conduct the animal experiments was obtained from the Lower Saxony State Office for Consumer Protection and Food Safety (approval no. 33.8-42502-04-20/3358) and all the experiments were conducted in strict compliance with European guidelines (EU directive on animal testing 2010/63/EU) and German Animal Welfare Law.

Mice

Four- to twelve-week-old female BALB/cAnNCrl (BALB/c) mice were purchased from Charles River Laboratories and were housed under specific pathogen-free conditions at the animal facility of the University of Veterinary Medicine Hannover, Foundation, in individually ventilated cages (type Sealsafe Plus GM500 or IsoCage N Biocontainment system; Tecniplast) for the entire duration of the experiment. All mice were taken into experiments after two weeks of acclimatization. Sterilized food pellets and water were provided *ad libitum*.

Viruses

Viral stocks of hRVFV-4s (vaccine strain), RVFV-4s_{GFP}, RVFV-Clone 13 and RVFV-35/74 (challenge strain) were provided by Wageningen Bioveterinary Research, The Netherlands, and generated as described previously [19,20].

Vaccination challenge study

Six-week-old female BALB/c mice ($n = 8$ per group) were immunized by intramuscular (i.m.) injections of $10^{5.8}$ TCID₅₀ of hRVFV-4s in 50 μ l of PBS as a single dose or in two doses at 28 d intervals. All control mice received 50 μ l of PBS at the same time and same protocol. At 21 days post single or booster dose, blood was drawn for serology by *vena facialis* puncture under isoflurane-induced anaesthesia and collected in MiniCollect® CAT Serum Sep Clot Activator tubes (Greiner Bio-One GmbH). At 28 days post single or booster dose, mice were challenged with 500 TCID₅₀ of virulent RVFV strain 35/74, which was delivered intraperitoneally (i.p.) in 100 μ l of PBS.

Adoptive transfer experiments

Six-week-old female BALB/c donor mice ($n = 16$ per group) were immunized by administering two doses of $10^{5.8}$ TCID₅₀ of hRVFV-4s i.m. at an interval of 28 days between each dose. All mock-immunized donor mice ($n = 16$) received PBS. Serum and spleens were collected from these mice 28 days after the booster dose was administered. Sera from the respective groups were pooled and 200 μ l was administered i.p. into ten to twelve-week-old naïve female BALB/c recipient mice ($n = 16$ per group). Similarly, splenocytes from each group were pooled and CD3⁺ T cells were isolated using the autoMACS® Pro Separator (Miltenyi Biotec B.V. & Co. KG) and the mouse Pan T Cell Isolation Kit II (Miltenyi Biotec B.V. & Co. KG). Approximately, $9\text{--}11 \times 10^6$ CD3⁺ T cells (>95% purity) were injected i.p. into 13- to 14-week old naïve recipient mice ($n = 16$ per group). Two hours post transfer of serum or T cells, the recipient mice were challenged i.p. with 500 TCID₅₀ RVFV strain 35/74. Following the challenge with RVFV strain 35/74 infection, mice were monitored daily for a period of 5 days for the development of clinical signs and were given clinical scores. A clinical scoring system has been established based on the appearance, activity, motility, body weights and presence of neurological symptoms. Humane endpoints (HEPs) were defined as the maximum clinical score attained in one of the given categories such as >20% weight loss, stupor, severe kyphosis and partial paresis of hind leg, or when a total clinical score of 9 is achieved. Mice attaining scores corresponding to HEPs were taken out of the experiment. The remaining mice were monitored until study endpoints (SEP) which is either 3 days post infection (dpi) or 5 dpi. Serum, liver and brain samples were collected and stored under appropriate conditions for further analysis.

Analysis of antibody and T cell responses

VN antibodies in the sera collected from mock and hRVFV-4s-immunized mice were assessed using

virus neutralization assays whereas the frequency of virus-specific T cells was estimated using mouse IFN- γ ELISpot assay and flow cytometry following restimulation of splenocytes with peptide pools spanning RVFV-N, Gn, Gc and NSm proteins. These methods are described in more detail in the supplementary methods.

RNA isolation and real time quantitative RT-PCR

Organs collected in screwcap tubes were homogenized on Tissue LyserII (Qiagen). Total RNA was isolated from cell debris-free organ homogenates using Mag-MaxTM mirVana total RNA isolation kit (Applied Biosystems) on an automated KingFisher Flex (ThermoFisher Scientific) according to the manufacturer's instructions. For detection of RVFV strain 35/74 RNA, real time quantitative reverse transcription (RT)-PCR using One-Step RT-PCR Kit (Qiagen) was performed using forward primer 5'-AAAGGAA-CAATGGACTCTGGTCA-3', reverse primer 5'-CACTTCTTACTACCATGTCCTCCAAT-3' and probe 5'-6FAMVWRAAAGC-TTGTATATCTCT-CAGTGCCCAATMR-3' published by Drosten *et al.* [21]. Ten-fold serial dilution of RVFV-M segment-specific RNA standard was used to generate a standard curve. Real time quantitative RT-PCR was performed in duplicates using Bio-Rad CFX96 real-time system (Bio-Rad) and viral RNA copies/gram of tissue were calculated from the obtained Cq values.

Histology and immunohistochemistry

Liver and brain tissue samples of all mice were fixed in ROTI[®]Histofix 4% (4% formaldehyde, Roth) for a minimum of two weeks. Two sections of the liver (left lateral lobe, right lateral lobe) and two longitudinal sections of the right hemisphere of the brain were stained with haematoxylin and eosin (HE) for histopathological evaluation. Immunohistochemistry (IHC) was performed using a polyclonal antibody targeting RVFV nucleocapsid (N) (1:400, GenScript) as previously described [22]. A semiquantitative scoring system was applied for HE-stained sections and IHC evaluation of liver samples. Each liver lobe was scored according to the percentage of tissue affected by hepatocellular necrosis and by immunoreactivity for RVFV nucleocapsid (N) as follows: 1 "mild": > 0–25%; 2 "moderate": > 25–50%; 3 "severe/marked": > 50% affected liver tissue and a mean score of both was calculated subsequently. Due to only minor changes in the brain, this scoring system was not applicable and hence only qualitative histopathological and immunohistochemical analyses were performed.

Statistics

The data were analyzed using GraphPad Prism 9 (version 9.5.1). The onset of clinical signs and survival curves are displayed as Kaplan-Meier curves, tested by log-rank test. Two-way ANOVA with Dunnett's multiple-comparison test was used for statistical analysis unless otherwise stated. A *p*-value <0.05 was considered significant.

Results

hRVFV-4s vaccination protects mice against lethal RVFV infection

In accordance with previous studies, we independently confirm the protective efficacy of hRVFV-4s in a mouse model of lethal RVFV infection. As described in the scheme in Figure 1(A), mice (*n* = 8 per group) were either vaccinated by administering one or two doses of hRVFV-4s, or were mock-vaccinated (PBS) via the intramuscular route. All mock- and hRVFV-4s-vaccinated mice remained healthy throughout the vaccination period and gained body weight (Figure 1(B)). Following intraperitoneal (i.p.) challenge with virulent RVFV strain 35/74, seven of the eight mice in the mock-vaccinated control group displayed greater than 5% body weight loss at 3 dpi and other signs of disease like piloerection and/or reduced activity. In contrast, none of the hRVFV-4s-immunized mice displayed body weight loss or any clinical signs following infection (Figure 1(C & D)). At 3 dpi, half of the mice (*n* = 4) in each group were sacrificed irrespective of their clinical outcome and the organs were collected to assess viral loads. The remaining mice were further monitored until 5 dpi or were sacrificed when they reached HEPs. Among the remaining four mice, one mouse in the control group had inflammation in the left eye and succumbed to infection at 4 dpi. Two of the mice in the control group had a total clinical score of 2 and 6 due to weight loss, piloerection and reduced activity (Figure 1(D)). The remaining mouse in the control group displayed transient (>5%) body weight loss at 3 dpi but then regained weight later. Thereafter this mouse appeared healthy without displaying any clinical signs and survived until the study endpoint 5 dpi (Figure 1(D)). In contrast, all four remaining mice from the single dose and prime/boost hRVFV-4s-immunized groups did not display any clinical signs or body weight loss throughout the course of the experiment (Figure 1(C-E)).

Viral genome copy numbers were quantified in the liver and brain of mice sacrificed at 3 dpi, at HEPs or at 5 dpi. All affected mice from the control group had high viral RNA copy numbers in liver and brain. Notably, the single mouse in the control group without clinical signs also had high viral load in the liver but

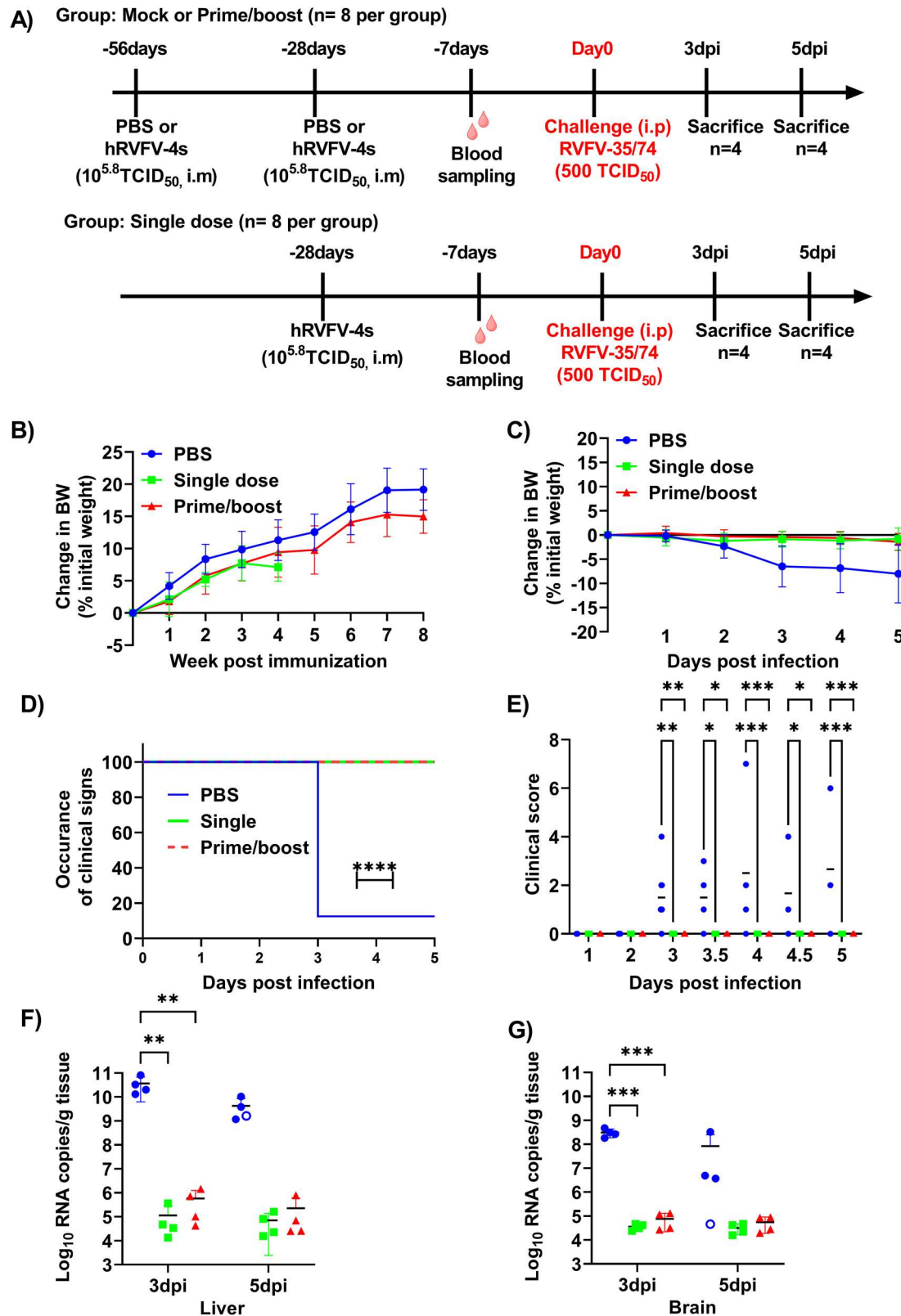


Figure 1. (A) Study design of the vaccination-challenge experiment. (B) Mean \pm SD of percentage changes in body weight of mock (blue line) and single dose (green line) or prime/boost (red line) hRVFV-4s-immunized mice after immunization and before challenge ($n = 8$ per group) (C) Mean \pm SD of percentage changes in body weight of mock (blue line) and single dose (green line) or prime/boost (red line) hRVFV-4s-immunized mice following challenge with RVFV strain 35/74. Body weight changes are relative to the measured weight just before the challenge and data correspond to $n = 8$ until 3 dpi and $n = 3-4$ for 4 and 5 dpi (D) Onset of clinical signs plotted for the mice from mock (blue line) single dose- (green) and prime boost-immunized (red) mice was monitored for a period of 5 days post RVFV 35/74 challenge (E) Comparison of the total clinical score of each mouse in mock (blue), single dose (green squares) and prime/boost (red triangles) groups at a given time point post infection until 5 dpi. * $p < 0.05$; ** $p < 0.01$; *** $p < 0.001$. Viral loads in liver (F) and brain (G) homogenates were determined by qPCR using RVFV-specific primer and probe set. The open circle in the figure represents the mouse in mock control that did not show clinical signs. Data corresponds to $n = 8$ for 3 dpi and $n = 4$ for 5 dpi. ** $p < 0.01$; *** $p < 0.001$.

not in the brain (Figure 1(F & G)). Viral RNA was also detected in the tissue homogenates of hRVFV-4s-immunized mice, although the copy numbers per gram tissue were significantly lower ($\sim 10^{4-5}$ times) compared to those of mock-immunized control mice (Figure 1(F & G)). No significant differences were observed in the viral RNA copy numbers between single dose and prime-boost groups.

Serum samples were subsequently analyzed for the presence of VN antibodies. A single immunization with hRVFV-4s induced VN antibodies titres ranging from 40 to 360 (median 240; $n = 6$) at day 21 post vaccination whereas the booster vaccination had significantly higher VN antibody titres and ranged from 1080 to as high as 29160 with a median value of 3240 (Figure 2(A)). Taken together, these findings confirm that a single dose hRVFV-4s immunization effectively induces protective immunity. Nevertheless, VN antibody responses can be enhanced by administering a second dose.

hRVFV-4s vaccination induces virus specific T cells

The two-dose vaccination regimen inducing stronger VN antibody responses was used for subsequent experiments to study correlates of protection. At 28 days after the second immunization, mice were sacrificed and approximately 10^7 splenocytes were used to determine the presence of RVFV-specific T cells by IFN- γ ELISpot assay. Splenocytes were stimulated with peptide pools spanning the N, NSm, Gc, and Gn proteins of RVFV. The results showed that immunization with hRVFV-4s induced strong RVFV-specific T cell responses, in particular to Gn (pool 1) and Gc (pool 2) glycoproteins. For other peptide pools, spanning the N and NSm proteins the response was below the baseline limit (Figure 2(B)). Furthermore, high numbers of IFN- γ^+ spot forming cells were also observed in hRVFV-4s-immunized mice following restimulation with RVFV-Clone 13 (Figure 2(B)). None of the mock-immunized control mice showed IFN- γ producing cells in response to any of the RVFV peptide pools or RVFV-Clone 13 restimulation (data not shown).

Furthermore, flow cytometry of splenocytes pooled from mock-immunized and hRVFV-4s-immunized mice and restimulated with peptide pools confirmed the presence of Gn- and Gc- specific T cells. Gn (pool 1) restimulation showed the presence of both CD4 $^+$ and CD8 $^+$ T cells producing IFN- γ and/or TNF- α in hRVFV-4s-vaccinated mice. In contrast, the IFN- γ^+ -producing cells that responded to the Gc (pool 2) restimulation, were predominantly CD8 $^+$ T cells. Restimulation with Clone 13 also activated both CD4 $^+$ and CD8 $^+$ T cells (Supplementary Figure S2).

Serum transfer studies

To determine whether antibodies afforded protection against RVFV disease, we performed passive transfer of serum harvested from control or hRVFV-4s-immunized mice into naïve recipient mice and subsequently challenged them with wild-type virus. A total of 13 of the 16 mice that received serum from mock-immunized donors succumbed to RVF disease at 3 dpi or had to be euthanized upon reaching an HEP. The remaining three mice in this group also displayed one or more clinical signs at 3 dpi with total clinical scores of 1, 2 and 5 (Figure 3(A)). Two of these mice were euthanized to assess viral loads in organs at 3 dpi whereas 1 mouse that was euthanized at 5 dpi displayed disease symptoms, including piloerection and greater than 5% body weight loss (total clinical score of 2). In contrast to the control mice, two out of 16 (12%) mice that received serum from hRVFV-4s-immunized mice succumbed to RVFV infection at 3 dpi (Figure 3(B)). Six of the 14 surviving hRVFV-4s serum recipient mice were euthanized at 3 dpi to assess viral loads. The remaining eight surviving hRVFV-4s serum recipient mice did not exhibit any signs of disease until the end of the experiment at 5 dpi.

Subsequent assessment of viral genome copy numbers in tissue homogenates showed 15 out of 16 control serum recipient mice presented with high viral loads (approximately 10^7 - 10^{11} RNA copies) in liver and brain tissues (Figure 3(C & D)). The data for one mouse was excluded from the analysis due to no Cq resulting from low total RNA concentration.

High viral load ($> 10^7$ RNA copies) was also detected in the two hRVFV-4s serum recipient mice that succumbed to the wild-type virus challenge at 3 dpi. Additionally, four mice in the hRVFV-4s serum recipient group also displayed high viral load ($> 10^6$ RNA copies) in the liver despite not displaying any signs of disease. Collectively, these results indicate that adoptive transfer of serum from hRVFV-4s-immunized mice affords recipient mice a substantial degree of protection against developing severe disease associated with RVFV infection.

CD3 $^+$ T cell adoptive transfer studies

To assess the contribution of RVFV-specific T cells to hRVFV-4s-induced protective immunity we adoptively transferred CD3 $^+$ T cells from spleens of either mock or hRVFV-4s-vaccinated donor mice into naïve recipients ($n = 16$) and subsequently challenged them with wild-type RVFV. Development of clinical signs was closely monitored up to 5 dpi. Mice that reached a HEP were euthanized. All 16 mice that had received T cells from mock-vaccinated donor mice and 14 mice that had received T cells from hRVFV-4s-vaccinated mice

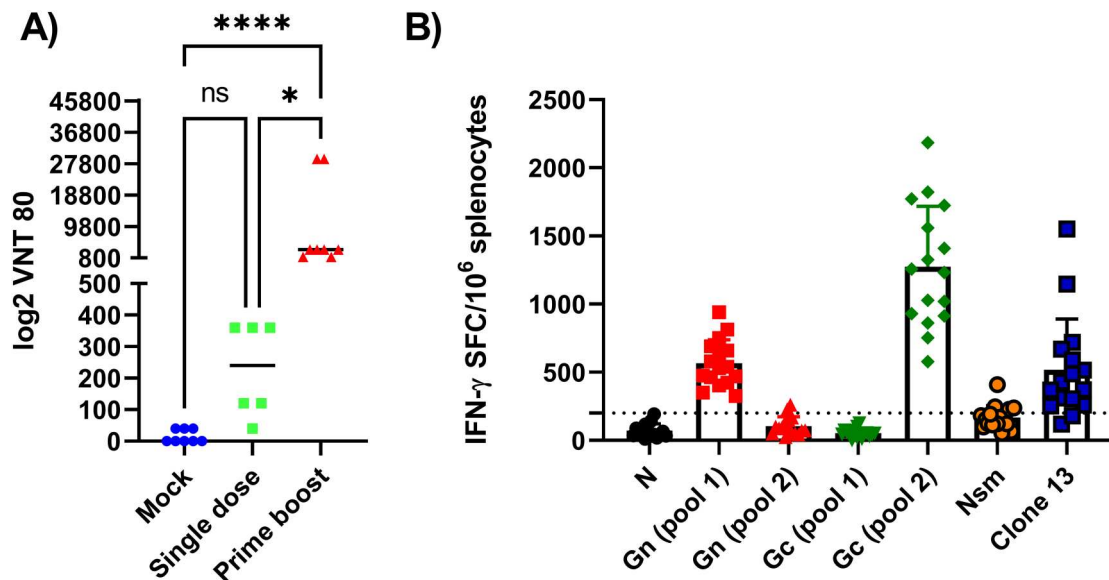


Figure 2. Virus-specific immune responses (A) Virus neutralization assay: The ability of immune sera collected from mock ($n = 8$; blue) single dose- ($n = 6$; green) or prime-boost-vaccinated mice ($n = 8$; red) to block RVFV-35/74-4s-eGFP infection of Vero E6 cells was tested. The GFP⁺ cells were counted on FLUOROSpot reader and the highest dilution at which cause 80% reduction in GFP⁺ cells was determined as virus neutralization titre (VNT₈₀). Each point represents a single mouse. The bars represent the mean value and the statistical analysis was performed using Kruskal Wallis test. * $p < 0.05$; **** $p < 0.0001$. (B) IFN- γ ELISPOT of splenocytes from hRVFV-4s-immunized mice ($n = 16$) restimulated with synthetic peptide pools corresponding to N, NSm, Gn and Gc proteins of RVFV. After, subtracting the background signal, the frequency of spot-forming cells (SFC) per million splenocytes was determined and plotted. Each data point represents the result obtained from a single mouse. The baseline is set to 100SFC/10⁶ splenocytes (dotted line) above which the response is considered positive.

displayed severe clinical signs and succumbed to the challenge infection between 3 and 5 dpi. Notably, two mice that received T cells from hRVFV-4s-vaccinated mice survived without any clinical signs until the end of the experiment (Figure 4(A)). As expected, all affected mice from both groups displayed high viral loads in the liver and brain whereas the two survivors from the hRVFV-4s recipient groups had viral RNA copy numbers that were several folds lower in both liver and brain (Figure 4(B)). These results indicate that RVFV-specific T cells may have afforded mice a limited degree of protection against lethal infection

with wild-type virus under these experimental conditions. However, the subtle difference observed between the recipients' T cells from mock- and hRVFV-4s-vaccinated donors did not reach statistical significance.

Histopathological and immunohistochemical examination of liver and brain

Histopathological changes in the liver comprised of randomly distributed, multifocal to diffuse hepatocellular necrosis (Figure 5(D & E)), mild

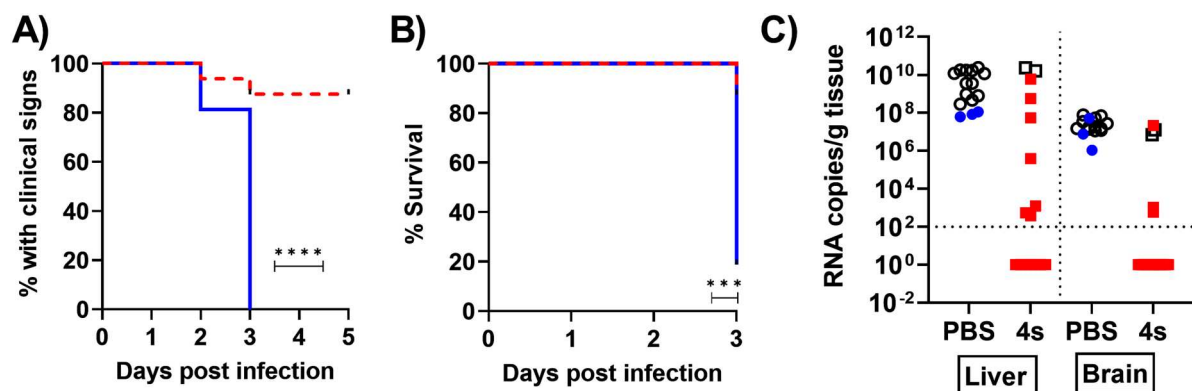


Figure 3. The appearance of clinical signs of disease (A) and survival rates (B) after RVFV 35/74 infection until 3 dpi was plotted for mice that received serum from mock-vaccinated (blue line) or hRVFV-4s-vaccinated (red dashed line) donor mice. The data corresponds to 16 mice per group until 3 dpi. For 4 and 5 dpi, $n = 1$ for PBS serum recipients and $n = 8$ for hRVFV-4s serum recipients. *** $p < 0.001$ and **** $p < 0.0001$ (C) Viral RNA copies are depicted per gram tissue detected in liver and brain of mock-vaccinated (circles) or hRVFV-4s-vaccinated (squares) serum recipients following RVFV 35/74 challenge. Filled symbols represent mice that were sacrificed either without or with less severe symptoms.

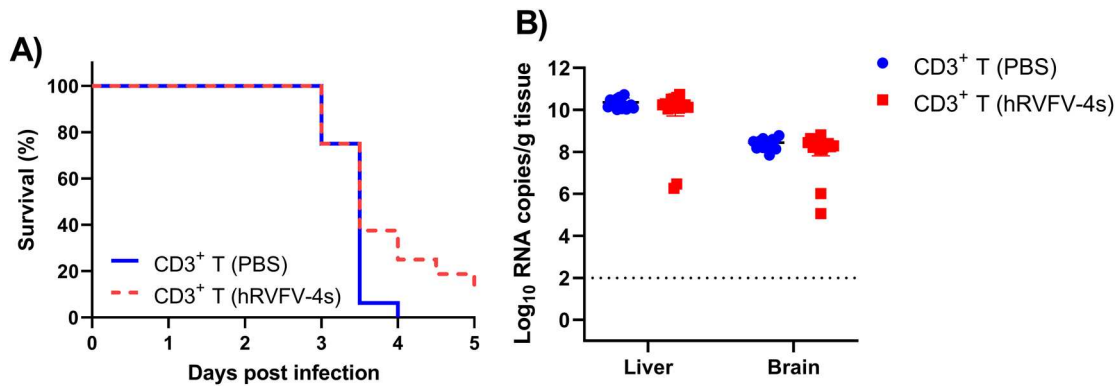


Figure 4. (A) Survival of recipient mice ($n = 16$) that received CD3⁺ T cells from mock- (blue line) or hRVFV-4s-vaccinated (red line) donor mice before they were challenged with RVFV strain 35/74. (B) After challenge with RVFV strain 35/74 viral RNA copies were quantified per gram of tissue from liver and brain homogenates of the recipients of CD3⁺ T cells from mock- (blue dots) or hRVFV-4s-vaccinated (red squares) donor mice.

lymphohistiocytic, periportal infiltrates, few necrotic foci with low numbers of infiltrating neutrophils, occasional hepatocellular cytoplasmic glycogen/lipid storage and frequently increased number of binucleated hepatocytes. In general, we found prominent histopathological changes in the liver of all the affected mice from the adoptive transfer experiment.

In 12 out of 16 mice that received serum from hRVFV-4s-vaccinated donors the HE liver score was 0 (Figure 5(A & C)); three mice exhibited a score of 3 and one mouse was scored with 1. Accordingly, staining for RVFV nucleocapsid antigen (N) confirmed the histopathological results with no detection of viral antigen in 12 out of 16 mice and the presence of viral antigen in the remaining four (Figure 5(B)).

The majority of mice (14/16) that received serum from mock-immunized donors displayed severe histopathological hepatic lesions with a score of 3, while the remaining two mice had less severe lesions with scores below 3 (Figure 5(A)). The majority of these mice (13/16) were characterized by marked immunoreactivity for RVFV nucleocapsid (N) with a score of 3, and 3 out of 16 mice exhibited a mild to moderate immunoreactivity for viral antigen (Figure 5(B & F)).

All CD3⁺ T cells recipient mice (n = 8/group) irrespective of whether T cells originated from mock-vaccinated or from hRVFV-4s-vaccinated donors showed severe liver lesions as well as marked immunoreactivity for RVFV nucleocapsid (N) in IHC (Figure 5(A & B)).

HE analysis of brain sections lacked significant microscopic lesions. In the brain of one mouse that received serum from mock-vaccinated donors, IHC for RVFV nucleocapsid (N) revealed cytoplasmic labelling of few, multifocal cells within the hypothalamus, most likely representing neurones (data not shown).

Discussion

In the present study, we have shown that the live-attenuated hRVFV-4s vaccine candidate elicits both

strong antibody and T cell responses in mice and confirmed that the vaccine affords protection against lethal challenge infection. Furthermore, we demonstrated that VN antibodies are a major correlate of protection in this lethal RVFV hepatic disease mouse model, whereas only limited protective effects of virus-specific T cells could be demonstrated. In line with all other pre-clinical results obtained so far [18,19] hRVFV-4s administration did not cause any adverse effects in this mouse model and all hRVFV-4s-vaccinated mice remained healthy throughout the immunization period.

Upon challenge infection with the highly virulent strain RVFV 35/74, BALB/c mice developed severe hepatic disease and the majority of infected mice succumbed within 3-5 dpi. Vaccination of mice with hRVFV-4s efficiently protected mice from developing severe hepatic disease upon challenge infection. These findings are in accordance with previous studies demonstrating the safety profile and protective efficacy of hRVFV-4s in ruminants and marmoset models of RVFV infection [17–19]. Mock-vaccinated mice had high viral loads in the liver and brain which were significantly lower in hRVFV-4s-vaccinated mice.

Administration of a single dose of the vaccine-induced VN antibodies, which were significantly boosted when a second dose was administered. Nevertheless, the protective efficacy achieved with both vaccination regimens was comparable. It was demonstrated recently that administration of small amounts of human monoclonal antibodies directed to the Gn protein affords BALB/c mice protection against RVFV ZH501 infection [23]. Furthermore, it has been shown that VN antibody titres >40 correlate with protection [24,25]. Therefore, VN antibody titres up to 360 induced with a single dose of hRVFV-4s might have been sufficient to protect mice against lethal RVFV infection. Most likely the VN antibodies induced after hRVFV-4s vaccination are directed to

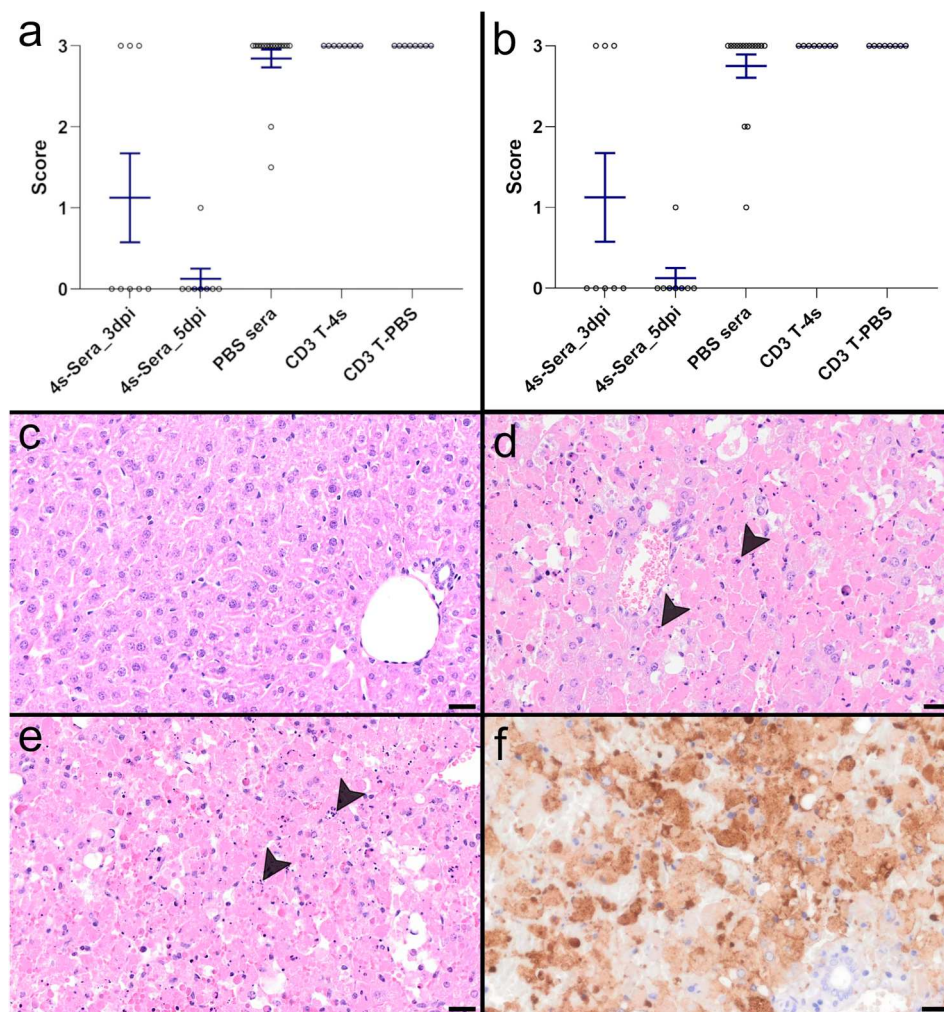


Figure 5. Histopathological and immunohistological analysis of liver: Graphs of (a) the histopathological scoring results of the haematoxylin and eosin (HE) stained liver sections and (b) the immunohistochemical scoring results of anti-RVFP nucleocapsid (N) stained liver sections. The x-axis displays the different groups, the y-axis the score with 0 = 0%; 1 “mild”: > 0–25%; 2 “moderate”: > 25–50%; 3 “severe/marked”: > 50% of liver tissue affected by hepatocellular necrosis (a) and of liver tissue immunopositive for RVFP antigen (b). Single dot plots display mean values (horizontal line) and standard error of the mean (vertical line). Each point represents the individual value of each animal examined. (c) Liver of a mouse that received serum from hRVFP-4s-vaccinated donors. No histopathological changes are visible in HE. (d) Liver of a mouse that received serum from mock-vaccinated donors showing severe hepatocellular necrosis with karyorrhectic, -lytic and pycnotic cell nuclei (arrowheads; score 3). (e) Liver of a mouse that received CD3+ T cells from hRVFP-4s-vaccinated donors displaying severe hepatocellular necrosis (arrowheads; score 3). (f) The liver of one of the mice that received serum from hRVFP-4s-vaccinated donors and showed high scores in HE and IHC in contrast to the majority of other mice from this group. IHC for anti-RVFP nucleocapsid (N) showing marked positive immunoreactivity of cells within the liver (score 3). Scale bars (c–e): 25 μ m; (f): 20 μ m.

the viral membrane glycoproteins Gn and Gc, because these proteins are crucial for virus attachment and fusion respectively [12–14].

To assess the relative contributions of antibody and T cell responses to protective immunity, we embarked on adoptive transfer experiments. Transfer of serum from hRVFP-4s-vaccinated donor mice prevented the development of severe disease in the majority of recipient mice following lethal challenge infection with RVFP. However, two mice that received hRVFP-4s immune serum developed severe disease and succumbed to the infection. Some mice had relatively high viral loads in liver in the absence of any clinical signs. Protection afforded by passive transfer of serum antibodies was not as robust as we observed

in the vaccination-challenge experiment where all hRVFP-4s-vaccinated mice had several fold lower viral load in organs compared to mock-vaccinated mice. It is likely that passive transfer of immune serum may not confer sterilizing immunity thus allowing virus replication in target organs.

hRVFP-4s vaccination also elicited a robust virus-specific T cell response, and flow cytometric analysis of splenocytes obtained from hRVFP-4s-vaccinated mice revealed the induction of both CD4⁺ and CD8⁺ T cells against Gc and Gn glycoproteins (Supplementary Figure 1). The adoptive transfer of RVFP-specific T cells afforded naïve recipient mice only modest protective immunity to challenge infection with RVFP strain 35/74. Two mice of this group survived the

infection until the study endpoint and also had lower viral loads in the brain and liver. However, the differences with the mice that received T cells from mock-vaccinated mice were not statistically significant. These findings are in concordance with another report that showed that T cell depletion from DelNSsRVFV-immunized mice before and after the challenge did not affect the protective efficacy of the vaccine [26]. Also in this study, passive transfer of immune sera was shown to be sufficient to confer protection to recipient mice [26]. The role of T cells in immunity to RVFV disease is less defined. Nevertheless, few reports suggest that T cells may have a critical role in protecting mice from developing encephalitis [15,27–29].

Histopathological analysis of tissue sections from the target organs further supported these findings. Notably, passive transfer of immune sera from hRVFV-4s-vaccinated donors prior to challenge infection prevented the establishment of infection in the target organs and protected most of the mice from subsequent hepatocellular damage. Nevertheless, all control recipient mice that either succumbed to infection or those that displayed high viral load in the liver had viral antigens and severe to moderate liver pathology. Interestingly most of the affected mice lacked profound lesions in the brain suggesting that these mice succumbed to severe hepatic disease.

The current infection model of rapid hepatic RVFV disease offers only a short time window for adoptively transferred virus-specific T cells to exert their protective effects. This might be the reason why a robust T cell response induced by hRVFV-4s immunization did not translate into protective efficacy. A slow progressing RVFV encephalitis model [30] might be more suitable for testing the protective efficacy of virus-specific T cells induced by hRVFV-4s vaccination. Nevertheless, the efficiency with which VN antibodies induced after hRVFV-4s vaccination protected mice from developing severe hepatic disease promotes the assessment of VN titres in future clinical trials.

The availability of safe and effective vaccines is crucial to prevent or mitigate the consequences of RVFV outbreaks. Thus, hRVFV-4s holds promise as a human RVFV vaccine candidate. The present study demonstrated that serum VN antibodies were the major hRVFV-4s-induced correlate of protection against lethal RVFV challenge, but the role of vaccine-induced T cells may have been undermined in this infection model due to rapid disease progression and requires further investigation. Also, studies investigating the longevity of immune responses and clinical testing of hRVFV-4s are warranted and currently conducted.

Acknowledgements

The authors would like to thank Dr. Marie Flamand from Institute Pasteur for providing the RVFV clone 13 used in

this study. The authors also thank Sonja Stelz, Leoni Engels, and Antonia Molle for their excellent technical support.

Disclosure statement

P.J.W.S. and J.K. are inventors of WIPO Patent Application WO/2014/189372 “Bunyaviruses with segmented glycoprotein genes and methods for generating these viruses”, owned by BunyaVax B.V. P.J.W.S. is non-executive Scientific Officer of BunyaVax. The remaining authors declare no competing interests.

Funding

This study is part of LARiSSA project funded by the Coalition for Epidemic Preparedness Innovations (CEPI) with support from the EU Horizon 2020 program. The study was partly supported by Alexander von Humboldt (AvH) Foundation in the framework of the AvH professorship endowed by the German Federal Ministry of Education and Research and the Deutsche Forschungsgemeinschaft (DFG, German research foundation- 398066876/GRK 2485/1. We acknowledge financial support by the Open Access Publication Fund of the University of Veterinary Medicine Hannover, Foundation.

Author contributions

CKP, JK, PWS, AO, and GFR conceptualized the study. CKP, GS, JF, LW, TG, JB, and MK performed the experiments. PWS and JK provided the viral stocks used in this study. IZ, CP, and WB performed histopathological analysis. Data analysis was done by CKP, IZ, GS, and CP. CKP, PWS, WB, IZ, AO, and GFR wrote and reviewed the manuscript. Funding for this study was acquired by AO, PWS, JK, and GFR.

ORCID

Chittappen K. Prajeeth  <http://orcid.org/0000-0002-6631-2096>

Isabel Zdora  <http://orcid.org/0000-0002-9926-0173>

Lucas Wilken  <http://orcid.org/0000-0002-5678-3089>

Jana Beicht  <http://orcid.org/0009-0004-7778-3928>

Jeroen Kortekaas  <http://orcid.org/0000-0002-0329-0176>

Paul J. Wichgers Schreur  <http://orcid.org/0000-0001-9790-2438>

Albert D.M.E. Osterhaus  <http://orcid.org/0000-0001-6535-3497>

Guus F. Rimmelzwaan  <http://orcid.org/0000-0002-1921-4581>

References

- [1] Nair N, Osterhaus A, Rimmelzwaan GF, et al. Rift Valley fever virus-infection, pathogenesis and host immune responses. *Pathogens*. 2023 Sep 19;12(9): e1174. doi:10.3390/pathogens12091174
- [2] Wright D, Kortekaas J, Bowden TA, et al. Rift Valley fever: biology and epidemiology. *J Gen Virol*. 2019 Aug;100(8):1187–1199. doi:10.1099/jgv.0.001296

- [3] Ikegami T, Makino S. The pathogenesis of Rift Valley fever. *Viruses*. 2011 May;3(5):493–519. doi:10.3390/v3050493
- [4] von Teichman B, Engelbrecht A, Zulu G, et al. Safety and efficacy of Rift Valley fever Smithburn and Clone 13 vaccines in calves. *Vaccine*. 2011 Aug 5;29(34):5771–5777. doi:10.1016/j.vaccine.2011.05.055
- [5] Dungu B, Louw I, Lubisi A, et al. Evaluation of the efficacy and safety of the Rift Valley fever Clone 13 vaccine in sheep. *Vaccine*. 2010 Jun 23;28(29):4581–4587. doi:10.1016/j.vaccine.2010.04.085
- [6] Makoschey B, van Kilsdonk E, Hubers WR, et al. Rift Valley fever vaccine virus clone 13 is able to cross the ovine placental barrier associated with foetal infections, malformations, and stillbirths. *PLoS Negl Trop Dis*. 2016 Mar;10(3):e0004550. doi:10.1371/journal.pntd.0004550
- [7] Kading RC, Crabtree MB, Bird BH, et al. Deletion of the NSm virulence gene of Rift Valley fever virus inhibits virus replication in and dissemination from the midgut of mosquitoes. *Plos Neglect Trop D*. 2014 Feb;8(2):e2670. doi:10.1371/journal.pntd.0002670
- [8] Weingartl HM, Zhang SZ, Marszal P, et al. Rift Valley fever virus incorporates the 78 kDa glycoprotein into virions matured in mosquito C6/36 cells. *PLoS One*. 2014 Jan 28;9(1):e87385. doi:10.1371/journal.pone.0087385
- [9] Kreher F, Tamietti C, Gomet C, et al. The Rift Valley fever accessory proteins NSm and P78/NSm-G are distinct determinants of virus propagation in vertebrate and invertebrate hosts. *Emerg Microbes Infect*. 2014 Oct 1;3:e71. doi:10.1038/emi.2014.71
- [10] Won SY, Ikegami T, Peters CJ, et al. NSm protein of Rift Valley fever virus suppresses virus-induced apoptosis. *J Virol*. 2007 Dec;81(24):13335–13345. doi:10.1128/JVI.01238-07
- [11] Ikegami T, Narayanan K, Won S, et al. Rift Valley fever virus NSs protein promotes post-transcriptional downregulation of protein kinase PKR and inhibits eIF2alpha phosphorylation. *PLoS Pathog*. 2009 Feb;5(2):e1000287. doi:10.1371/journal.ppat.1000287
- [12] Bian T, Hao M, Zhao X, et al. A Rift Valley fever mRNA vaccine elicits strong immune responses in mice and rhesus macaques. *NPJ Vaccines*. 2023 Oct 27;8(1):164. doi:10.1038/s41541-023-00763-2
- [13] Bian T, Wang B, Fu G, et al. Single-dose of a replication-competent adenovirus-vectored vaccine provides sterilizing protection against Rift Valley fever virus challenge. *Front Immunol*. 2022;13:907675. doi:10.3389/fimmu.2022.907675
- [14] Wright D, Allen ER, Clark MHA, et al. Naturally acquired Rift Valley fever virus neutralizing antibodies predominantly target the Gn glycoprotein. *Iscience*. 2020 Nov 20;23(11):e101669. doi:10.1016/j.isci.2020.101669
- [15] Harmon JR, Spengler JR, Coleman-McCray JD, et al. CD4 T cells, CD8 T cells, and monocytes coordinate to prevent rift valley fever virus encephalitis. *J Virol*. 2018 Dec;92(24):e1270. doi:10.1128/JVI.01270-18
- [16] Wichgers Schreur PJ, Oreshkova N, Moormann RJ, et al. Creation of Rift Valley fever viruses with four-segmented genomes reveals flexibility in bunyavirus genome packaging. *J Virol*. 2014 Sep;88(18):10883–10893. doi:10.1128/JVI.00961-14
- [17] Wichgers Schreur PJ, Mooij P, Koopman G, et al. Safety and immunogenicity of four-segmented Rift Valley fever virus in the common marmoset. *NPJ Vaccines*. 2022 May 18;7(1):54. doi:10.1038/s41541-022-00476-y
- [18] Wichgers Schreur PJ, Oreshkova N, van Keulen L, et al. Safety and efficacy of four-segmented Rift Valley fever virus in young sheep, goats and cattle. *NPJ Vaccines*. 2020;5(1):65. doi:10.1038/s41541-020-00212-4
- [19] Wichgers Schreur PJ, van Keulen L, Kant J, et al. Four-segmented Rift Valley fever virus-based vaccines can be applied safely in ewes during pregnancy. *Vaccine*. 2017 May 25;35(23):3123–3128. doi:10.1016/j.vaccine.2017.04.024
- [20] Bron GM, Schreur PJW, de Jong MCM, et al. Quantifying Rift Valley fever virus transmission efficiency in a lamb-mosquito-lamb model. *Front Cell Infect Mi*. 2023 Dec 18;13:e1206089.
- [21] Drosten C, Götting S, Schilling S, et al. Rapid detection and quantification of RNA of Ebola and Marburg viruses, Lassa virus, Crimean-Congo hemorrhagic fever virus, Rift Valley fever virus, Dengue virus, and Yellow fever virus by real-time reverse transcription-PCR. *J Clin Microbiol*. 2002 Jul;40(7):2323–2330. doi:10.1128/JCM.40.7.2323-2330.2002
- [22] Michaely LM, Rissmann M, Keller M, et al. NSG-Mice Reveal the importance of a functional innate and adaptive immune response to overcome RVFV infection. *Viruses*. 2022 Feb 8;14(2):e350. doi:10.3390/v14020350
- [23] Chapman NS, Hulswit RJG, Westover JLB, et al. Multifunctional human monoclonal antibody combination mediates protection against Rift Valley fever virus at low doses. *Nat Commun*. 2023 Sep 13;14(1):5650. doi:10.1038/s41467-023-41171-3
- [24] Pittman PR, Liu CT, Cannon TL, et al. Immunogenicity of an inactivated Rift Valley fever vaccine in humans: a 12-year experience. *Vaccine*. 1999 Aug 20;18(1-2):181–189. doi:10.1016/S0264-410X(99)00218-2
- [25] Papin JF, Verardi PH, Jones LA, et al. Recombinant Rift Valley fever vaccines induce protective levels of antibody in baboons and resistance to lethal challenge in mice. *P Natl Acad Sci USA*. 2011 Sep 6;108(36):14926–14931. doi:10.1073/pnas.1112149108
- [26] Doyle JD, Barbeau DJ, Cartwright HN, et al. Immune correlates of protection following Rift Valley fever virus vaccination. *Npj Vaccines*. 2022 Oct 28;7(1):e551. doi:10.1038/s41541-022-00551-4
- [27] Barbeau DJ, Cartwright HN, Harmon JR, et al. Identification and characterization of Rift Valley fever virus-specific T cells reveals a dependence on CD40/CD40L interactions for prevention of encephalitis. *J Virol*. 2021 Dec;95(23):e1506. doi:10.1128/JVI.01506-21
- [28] Dodd KA, McElroy AK, Jones MEB, et al. Rift Valley fever virus clearance and protection from neurologic disease are dependent on CD4 T cell and virus-specific antibody responses. *J Virol*. 2013 Jun;87(11):6161–6171. doi:10.1128/JVI.00337-13
- [29] Dodd KA, McElroy AK, Jones TL, et al. Rift Valley fever virus encephalitis is associated with an ineffective systemic immune response and activated T cell infiltration into the CNS in an immunocompetent mouse model. *Plos Neglect Trop D*. 2014 Jun;8(6):e2874.
- [30] Michaely LM, Schuwerk L, Allnoch L, et al. Intact type I interferon receptor signaling prevents hepatocellular necrosis but not encephalitis in a dose-dependent manner in Rift Valley fever virus infected mice. *Int J Mol Sci*. 2022 Oct 18;23(20):e12492. doi:10.3390/ijms232012492